

# Deep-blue supercontinnum sources with optimum taper profiles – verification of GAM

**Sørensen, Simon Toft; Møller, Uffe; Larsen, Casper; Moselund, P. M. ; Jakobsen, C. ; Johansen, J. ; Andersen, T. V. ; Thomsen, C. L. ; Bang, Ole**

*Published in:*
Optics Express

*Link to article, DOI:*
10.1364/OE.20.010635

*Publication date:*
2012

*Document Version*
Publisher's PDF, also known as Version of record

# Deep-blue supercontinnum sources with optimum taper profiles – verification of GAM

**S. T. Sørensen,[1,*] U. Møller,[1] C. Larsen,[1] P. M. Moselund,[2] C. Jakobsen,[2] J. Johansen,[2] T. V. Andersen,[2] C. L. Thomsen,[2] and O. Bang[1,2]**

[1]*DTU Fotonik, Department of Photonics Engineering, Technical University of Denmark, 2800 Kgs. Lyngby, Denmark*

[2]*NKT Photonics A/S, Blokken 84, DK-3460, Birkerød, Denmark*

[*]*stso@fotonik.dtu.dk*

**Abstract:** We use an asymmetric 2 m draw-tower photonic crystal fiber taper to demonstrate that the taper profile needs careful optimisation if you want to develop a supercontinuum light source with as much power as possible in the blue edge of the spectrum. In particular we show, that for a given taper length, the downtapering should be as long as possible. We argue how this may be explained by the concept of group-acceleration mismatch (GAM) and we confirm the results using conventional symmetrical short tapers made on a taper station, which have varying downtapering lengths.



**OCIS codes:** (060.4370) Nonlinear optics, fibers; (060.5295) Photonic crystal fibers; (320.6629) Supercontinuum generation.

## References and links

1. J. M. Dudley and J. R. Taylor, "Ten years of nonlinear optics in photonic crystal fibre," Nat. Photonics **3**, 85–90 (2009).
2. J. C. Knight, T. A. Birks, P. S. J. Russell, and D. M. Atkin, "All-silica single-mode optical fiber with photonic crystal cladding," Opt. Lett. **21**, 1547–1549 (1996).
3. P. Russel, "Photonic crystal fiber," Science **299**, 358–362 (2003).
4. J. Herrmann, U. Griebner, N. Zhavoronkov, A. Husakou, D. Nickel, J. C. Knight, W. J. Wadsworth, P. S. J. Russell, and G. Korn, "Experimental evidence for supercontinuum generation by fission of higher-order solitons in photonic fibers," Phys. Rev. Lett. **88**, 173901 (2002).
5. T. A. Birks, J. C. Knight, and P. S. Russell, "Endlessly single-mode photonic crystal fiber," Opt. Lett. **22**, 961–963 (1997).
6. J. C. Knight, "Photonic crystal fibres," Nature **424**, 847–851 (2003).
7. A. V. Husakou and J. Herrmann, "Supercontinuum generation of higher-order solitons by fission in photonic crystal fibers," Phys. Rev. Lett. **87**, 203901 (2001).
8. D. V. Skryabin, F. Luan, J. C. Knight, and P. S. J. Russell, "Soliton self-frequency shift cancellation in photonic crystal fibers," Science **301**, 1705–1708 (2003).
9. A. V. Gorbach and D. V. Skryabin, "Theory of radiation trapping by the accelerating solitons in optical fibers," Phys. Rev. A **76**, 053803 (2007).
10. A. V. Gorbach and D. V. Skryabin, "Light trapping in gravity-like potentials and expansion of supercontinuum spectra in photonic-crystal fibres," Nat. Photonics **1**, 653–657 (2007).
11. M. N. Islam, G. Sucha, I. Bar-Joseph, M. Wegener, J. P. Gordon, and D. S. Chemla, "Femtosecond distributed soliton spectrum in fibers," J. Opt. Soc. Am. B **6**, 1149–1158 (1989).
12. M. H. Frosz, O. Bang, and A. Bjarklev, "Soliton collision and raman gain regimes in continuous-wave pumped supercontinuum generation," Opt. Express **14**, 9391–9407 (2006).
13. D. R. Solli, C. Ropers, P. Koonath, and B. Jalali, "Optical rogue waves," Nature **450**, 1054–1057 (2007).

#161502 - $15.00 USD Received 13 Jan 2012; revised 26 Mar 2012; accepted 18 Apr 2012; published 24 Apr 2012

14. J. M. Dudley, G. Genty, and B. J. Eggleton, "Harnessing and control of optical rogue waves in supercontinuum generation," Opt. Express **16**, 3644–3651 (2008).
15. D. R. Solli, C. Ropers, and B. Jalali, "Active control of rogue waves for stimulated supercontinuum generation," Phys. Rev. Lett. **101**, 233902 (2008).
16. O. Bang and M. Peyrard, "Generation of high-energy localized vibrational modes in nonlinear klein-gordon lattices," Phys. Rev. E **53**, 4143–4152 (1996).
17. N. Akhmediev, J. M. Soto-Crespo, and A. Ankiewicz, "Could rogue waves be used as efficient weapons against enemy ships?" Eur. Phys. J. Special Topics **185**, 259–266 (2010).
18. P. Beaud, W. Hodel, B. Zysset, and H. P. Weber, "Ultrashort pulse propagation, pulse breakup, and fundamental soliton formation in a single-mode optical fiber," IEEE J. Quantum Elect. **23**, 1938–1946 (1987).
19. J. M. Stone and J. C. Knight, "Visibly "white" light generation in uniformphotonic crystal fiber using a microchip laser," Opt. Express **16**, 2670–2675 (2008).
20. A. V. Gorbach, D. V. Skryabin, J. M. Stone, and J. C. Knight, "Four-wave mixing of solitons with radiation and quasi-nondispersive wave packets at the short-wavelength edge of a supercontinuum," Opt. Express **14**, 9854–9863 (2006).
21. S. T. Sørensen, A. Judge, C. L. Thomsen, and O. Bang, "Optimum fiber tapers for increasing the power in the blue edge of a supercontinuum—group-acceleration matching," Opt. Lett. **36**, 816–818 (2011).
22. J. C. Travers and J. R. Taylor, "Soliton trapping of dispersive waves in tapered optical fibers," Opt. Lett. **34**, 115–117 (2009).
23. T. Schreiber, T. Andersen, D. Schimpf, J. Limpert, and A. Tünnermann, "Supercontinuum generation by femtosecond single and dual wavelength pumping in photonic crystal fibers with two zero dispersion wavelengths," Opt. Express **13**, 9556–9569 (2005).
24. S. Pricking and H. Giessen, "Tailoring the soliton and supercontinuum dynamics by engineering the profile of tapered fibers," Opt. Express **18**, 20151–20163 (2010).
25. J. C. Travers, "Blue extension of optical fibre supercontinuum generation," J. Opt. **12**, 113001 (2010).
26. J. M. Dudley, G. Genty, and S. Coen, "Supercontinuum generation in photonic crystal fiber," Rev. Mod. Phys. **78**, 1135–1184 (2006).
27. C. Agger, C. Petersen, S. Dupont, H. Steffensen, J. K. Lyngsø, C. L. Thomsen, J. Thøgersen, S. R. Keiding, and O. Bang, "Supercontinuum generation in zblan fibers—detailed comparison between measurement and simulation," J. Opt. Soc. Am. B **29**, 635–645 (2012).
28. T. A. Birks, W. J. Wadsworth, and P. S. J. Russell, "Supercontinuum generation in tapered fibers," Opt. Lett. **25**, 1415–1417 (2000).
29. S. Leon-Saval, T. Birks, W. Wadsworth, P. S. J. Russell, and M. Mason, "Supercontinuum generation in submicron fibre waveguides," Opt. Express **12**, 2864–2869 (2004).
30. F. Lu, Y. Deng, and W. H. Knox, "Generation of broadband femtosecond visible pulses in dispersion-micromanaged holey fibers," Opt. Lett. **30**, 1566–1568 (2005).
31. P. Falk, M. Frosz, and O. Bang, "Supercontinuum generation in a photonic crystal fiber with two zero-dispersion wavelengths tapered to normal dispersion at all wavelengths," Opt. Express **13**, 7535–7540 (2005).
32. A. Kudlinski, A. K. George, J. C. Knight, J. C. Travers, A. B. Rulkov, S. V. Popov, and J. R. Taylor, "Zero-dispersion wavelength decreasing photonic crystal fibers for ultraviolet-extended supercontinuum generation," Opt. Express **14**, 5715–5722 (2006).
33. J. C. Travers, J. M. Stone, A. B. Rulkov, B. A. Cumberland, A. K. George, S. V. Popov, J. C. Knight, and J. R. Taylor, "Optical pulse compression in dispersion decreasing photonic crystal fiber," Opt. Express **15**, 13203–13211 (2007).
34. A. Kudlinski and A. Mussot, "Visible cw-pumped supercontinuum," Opt. Lett. **33**, 2407–2409 (2008).
35. A. Kudlinski, M. Lelek, B. Barviau, L. Audry, and A. Mussot, "Efficient blue conversion from a 1064 nm microchip laser in long photonic crystal fiber tapers for fluorescence microscopy," Opt. Express **18**, 16640–16645 (2010).
36. J. Cascante-Vindas, A. Díez, J. L. Cruz, and M. Andrés, "White light supercontinuum generation in a y-shaped microstructured tapered fiber pumped at 1064 nm," Opt. Express **18**, 14535–14540 (2010).
37. M. Liao, W. Gao, Z. Duan, X. Yan, T. Suzuki, and Y. Ohishi, "Directly draw highly nonlinear tellurite microstructured fiber with diameter varying sharply in a short fiber length," Opt. Express **20**, 1141–1150 (2012).
38. S. P. Stark, J. C. Travers, and P. S. J. Russell, "Extreme supercontinuum generation to the deep uv," Opt. Lett. **37**, 770–772 (2012).
39. N. Vukovic, N. Broderick, M. Petrovich, and G. Brambilla, "Novel method for the fabrication of long optical fiber tapers," IEEE Photon. Technol. Lett. **20**, 1264–1266 (2008).
40. P. Falk, M. H. Frosz, O. Bang, L. Thrane, P. E. Andersen, A. O. Bjarklev, K. P. Hansen, and J. Broeng, "Broadband light generation at 1300 nm through spectrally recoiled solitons and dispersive waves," Opt. Lett. **33**, 621–623 (2008).
41. M. Koshiba and K. Saitoh, "Applicability of classical optical fiber theories to holey fibers," Opt. Lett. **29**, 1739–1741 (2004).

#161502 - $15.00 USD Received 13 Jan 2012; revised 26 Mar 2012; accepted 18 Apr 2012; published 24 Apr 2012

## 1. Introduction

Supercontinuum (SC) generation is a striking phenomenon of extreme spectral broadening involving a wealth of beautiful nonlinear physics [1]. Although being first observed in bulk glass and later studied in telecom optical fibers, the study of SC generation and the development of today's commercial SC sources first really took off with the invention of the photonic crystal fiber (PCF) [2], in which light can be manipulated by air-hole structuring [3]. The study of SC generation is inherently linked to the fundamental field of soliton physics and due to the striking efficiency of SC generation in PCFs, researchers have been able to reveal numerous new and important fundamental effects and surprising links with other physical systems. The advent of the PCF therefore spawned a re-birth of not only SC generation, but nonlinear fiber optics in general [1], due to the tremendous degree of design freedom that has enabled engineers to push the properties of PCFs to limits that could never have been achieved with standard optical fibers or in bulk materials [3]. For example, one can move their zero-dispersion wavelength (ZDW) down in the visible [4], make them endlessly single-moded [5], and even make them guide light in air [6]. The PCF further enabled the discovery of several fundamental nonlinear phenomena, such as soliton fission [7], Raman redshift cancellation by the presence of a second ZDW [8], soliton trapping of dispersive waves (DWs) in gravitational wells [9, 10], generation of large-amplitude optical rogue waves [11–13] and the control of rogue waves by minute seeds [14,15]. Rogue waves are in fact a fundamental nonlinear phenomenon generated by soliton collision in nonlinear physical models [16]. Thus they appear in such diverse systems as ocean waves, where they appear out of nowhere and cause serious damage on ships [17], and in biology, where they are known as "highly localized modes" that break the bonds in DNA and initiate DNA denaturation [16].

SC generation involves the full scale of soliton physics and thus all the above mentioned effects; even rogue waves appear in the form of mega solitons that are subject to large Raman redshifts and thus define the long-wavelength "red" spectral edge of the SC. This in turn defines the short-wavelength "blue" edge through a complex trapping mechanism that manifests itself as a lock between the two edges; when the solitons at the red edge are redshifted by the Raman effect, they push the DWs at the blue edge to shorter wavelengths in a way that satisfies group-velocity (GV) matching [18,19]. The blueshift of a DW package has been explained as a cascade of cross-phase modulation (XPM) collision events that continuously blueshifts the DW package in discrete steps [20]. Alternatively, the trapping can be elegantly explained as an effect imposed by the accelerating soliton that sets up a gravitational well around the DW package and prevents it from dispersing [9,10]. The trapping effect is of fundamental importance for the SC generation dynamics, and GV matching is hence of equal importance to ensure a continued interaction between the spectral components in the normal and anomalous dispersion regime, and thereby allowing generation of SC spectra with a blue edge reaching into the ultraviolet below 400 nm.

A topic that has so far remained largely uninvestigated is the consequences of the fact that the trapping is not complete: the DWs continuously loose energy. The solitons undergo a continuous Raman redshift, which leads to a continuous change in GV with propagation length, i.e. a *group-acceleration*, but the DWs do not in their own right move spectrally and are thus not subject to the same acceleration. This means that there is continuously a small difference in GV, and thus a constant small leakage of DW energy, as illustrated in Fig. 1(a). The Raman effect thus leads to a *group-acceleration mismatch* (GAM), an asymmetric change in the group-acceleration of the solitons and DWs [21]. The effect is not significant in uniform fibers, because the weak redshift leads only to a minor GAM. However, in a fiber taper the group-acceleration can be orders of magnitude larger than the inherent Raman induced change and it is generally highly asymmetric, in the sense that the taper-induced shift in GV at the DW wave-

#161502 - $15.00 USD Received 13 Jan 2012; revised 26 Mar 2012; accepted 18 Apr 2012; published 24 Apr 2012

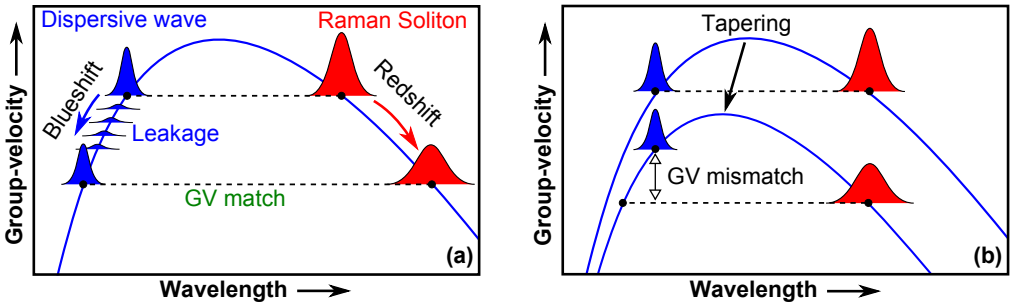


Fig. 1. Radiation trapping and leakage. (a) In a uniform fiber a soliton can trap and blueshift a GV matched DW, while it is slowly redshifting and thus decelerating. The trapping is incomplete, i.e. part of the DW continuously leaks out of the trap, as illustrated. (b) In a taper, there is an asymmetric change in GV of the soliton and trapped DW. That is, there is a mismatch in the group-acceleration, the rate with which the GV changes, which increases the amount of light that leaks out of the trap (not illustrated). In the figure it is assumed that the dispersion increases for the soliton both when it is redshifted and when the fiber is tapered.

length is much smaller than at the longer soliton wavelength, as illustrated in Fig. 1(b) and for the real fiber tapers used in this work. In [22] it was demonstrated that the group-acceleration in a taper can in fact supply the needed soliton deceleration to trap a DW even in the absence of the Raman effect. In physical terms, the GAM lowers the XPM interaction length, whereas in the trapping picture GAM lowers the depth of the gravitational well, causing light to escape. It has been demonstrated in [23] that light can escape or pass unaffected through the XPM interaction region in the extreme case when the interaction length is very short, i.e., when the GV difference is very large.

In this work, we investigate the influence of the enforced asymmetry in the group-acceleration of the solitons and trapped DWs in tapered PCFs. The influence of the taper shape on the spectrum was investigated in [24], where short femtosecond pulses were launched directly into ultra-short tapers to push the pulse break-up into the tapered part of the fiber. Although interesting, the results in [24] describe a dynamical regime different from that typical of long-pulsed commercial SC systems investigated this work, where long tapers are used and where MI breaks up the long pulse into a large number of fundamental solitons and not higher-order solitons. First we illustrate the fundamental physics behind GAM with numerical simulations of the propagation of a single soliton and GV matched DW in a taper. We then present experimental results of high-power SC generation in tapered PCFs of varying lengths and shapes. In particular, we experimentally demonstrate for the first time that the length of the downtapering section has a major impact on the available power in the blue edge of the spectrum, which provide the first clear evidence of the importance of GAM. The results provide the first step towards determining the optimum shape of a fiber taper for deep-blue supercontinuum sources, which has so-far remained largely unknown [25].

## 2. Numerical results

In [19, 25] it was shown how the position of the blue edge can be accurately predicted from the dispersion characteristics of any given fiber. The red edge is ultimately limited by the silica loss edge starting at 2200-2400 nm, and the position of the blue edge is then determined by GV matching with the red edge. Although useful for tailoring the spectral width, this does not give any information on the available spectral density in the blue edge of the SC.

#161502 - $15.00 USD Received 13 Jan 2012; revised 26 Mar 2012; accepted 18 Apr 2012; published 24 Apr 2012

At a first glance, the SC dynamics may seem overwhelmingly complicated. However, due to the solitonic nature of SC generation, one can gain a lot of insight into the basic dynamics on the basis of single soliton simulations. It is particularly illustrative to neglect the central part of the SC and treat only the edges. To get a basic understanding of the SC generation in a tapered fiber, it will hence suffice to analyse the propagation of a soliton and appropriately delayed and GV matched DW package. Here we do this by numerical modelling of the generalised nonlinear Schrödinger equation, which is often utilised to aid the understanding of the dynamics, and has successfully been demonstrated to accurately reproduce experimental results in both silica [26] and soft-glass fibers [27].

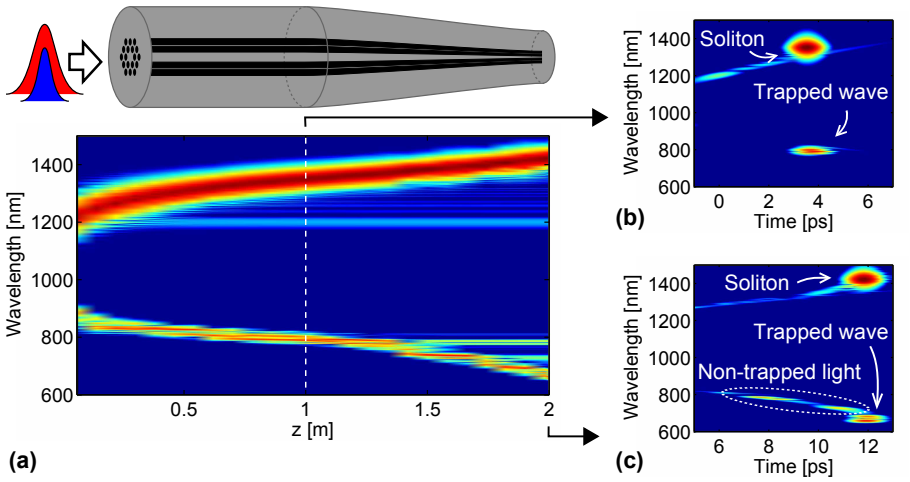


Fig. 2. (a) Spectral evolution of a 20 fs fundamental soliton and trapped wave through a fiber taper with an initial 1 m uniform fiber. (b)-(c) Spectrograms at the entrance (1 m) of the taper and at the taper waist (2 m). The wave is fully trapped at the taper entrance, but the taper increases the soliton redshift and deceleration, which causes light to leak from the soliton induced trapping region.

The propagation of a 20 fs fundamental soliton and GV matched DW in Fig. 2(a) illustrates the basic dynamics in a tapered fiber: the soliton redshifts throughout the length of the fiber, and while doing so, it causes a blueshift of the trapped wave. In the first meter of uniform fiber, the two co-propagate without the DW shedding much energy. As the downtapering starts at 1 m, both the redshift rate of the soliton and the blueshift rate of the trapped wave increase due to the increase in nonlinearity and change in GV. However, due to the taper induced GAM, a significant fraction of the trapped DW escapes the trap. The spectrograms in Fig. 2(b)-2(c) show the pulses in the spectral and time-domain simultaneously; at the taper entrance (Fig. 2(b)), the two waves are temporally overlapping and the decelerating soliton has fully trapped the DW. At the taper end (Fig. 2(c)) only a fraction of the originally trapped DW is still trapped and has a temporal overlap with the soliton. The remaining light has escaped the trap and not been decelerated and blueshifted by the soliton. This clearly illustrates the need for matching not only the GVs but also the rate with which they change, i.e. the need for minimising the GAM as predicted numerically in [21].

## 3. Experimental results

To investigate the full scale importance of GAM on SC generation comprised by hundreds of solitons and DWs, we fabricated an asymmetric draw-tower taper. The asymmetry enforces a

#161502 - $15.00 USD Received 13 Jan 2012; revised 26 Mar 2012; accepted 18 Apr 2012; published 24 Apr 2012

difference in the GAM depending on whether the fiber is pumped from the long or short down-tapering side, while ensuring that the light passes through the same length of fiber. Tapering has previously been demonstrated as an effective way of manipulating the pulse propagation by changing the dispersion and increasing the effective nonlinearity, and thereby move the short-wavelength edge of an SC further into the blue [24, 25, 28–37]. Spectra extending down to 330 nm from a 1065 nm pump have been reported [25], and an impressive 280 nm was reached in [38] by pumping an ultrashort taper with a femtosecond pump at 800 nm. In the latter case the light was generated directly in the UV region by a completely different mechanism.

Unlike the draw-tower tapers presented in, e.g. [25,32–35,37], our taper is tapered back to its original diameter, which makes splicing and interfacing easier and allows for an investigation of the impact of the asymmetry. It has generally been the belief [39] that such tapers shorter than 10 m are difficult to fabricate on a draw-tower. On the contrary, we find that tapering directly on the draw-tower offers high accuracy of the fiber parameters by pressure control, and allows fabrication of accurate fiber tapers with lengths from a few meters and up. This further makes it possible to use the draw-tower's coating system as an integrated part of the taper fabrication. A very short draw-tower taper of only 10 cm was recently fabricated in [37] showing the flexibility of draw-tower tapering.

As an additional investigation of the influence of the taper shape on the spectrum, we fabricated three ultra-short tapers using a well-known post-processing technique on a tapering station (Vytran LDS-1250). This technique limits the length of the tapered section to around 15 cm.

The draw-tower taper was based on the commercial fiber SC-5.0-1040 from NKT Photonics A/S with a hole-to-pitch ratio of $d/\Lambda = 0.52$. In the tapered section its pitch was reduced from 3.3 to 2.5 $\mu$m. The ultra-short Vytran tapers were based on a standard fiber with a hole-to-pitch ratio of $d/\Lambda = 0.79$ and a pitch of $\Lambda = 3.7$ $\mu$m that was reduced by 50% in the tapered section. The dispersion and GV profiles are shown in Fig. 3 along with an illustration of how the optimum degree of tapering was determined: We define the red edge $\lambda_{\text{red}}$ as the loss edge $\lambda_{\text{loss}}$ (here set to 2300 nm), or a wavelength $\lambda_2$ close to the second ZDW, whichever is the lowest. Solitons always halt their redshift about 50-100 nm away from the 2nd ZDW [8, 40] so $\lambda_2$ is chosen to $\lambda_{\text{ZDW},2} - 50$ nm, which means that

$$\lambda_{\text{red}} = \min\{\lambda_{\text{loss}},\ \lambda_{\text{ZDW},2} - 50\ \text{nm}\}. \tag{1}$$

The red edge in turn defines the blue edge through GV matching, and the optimum degree of tapering is determined by finding the pitch at which GV matching is achieved to the shortest possible wavelength. In Fig. 3(c) and 3(f) we show the so defined red and blue edges together with both ZDWs. The optimum blue edge, i.e. shortest wavelength, is found at the turning point, which is for a pitch of 2.6 and 1.8 $\mu$m for the draw-tower and Vytran tapers, respectively, giving a blue edge of 476 and 378 nm, respectively. The realized pitch at the taper waist is very close to the optimum. In Fig. 4 we have plotted the optimum pitch and blue edge versus the relative hole size. We see that the optimum pitch approaches $\sim 1.8$ $\mu$m for increasing relative hole sizes, which corresponds to the point where the second ZDW crosses the loss edge, as can be seen from Fig. 3(f). For smaller relative hole sizes, where the optimum pitch is larger than 2 $\mu$m, the optimum is obtained before the second ZDW has crossed the loss edge. We emphasize that the fibers used in this work are not the optimum in terms of generating light at the shortest possible wavelength. The focus in this work is on how to maximise the amount of light in the blue edge, and we therefore chose a fiber with $d/\Lambda = 0.52$ because it is single-moded at the pump [41].

The blue edge versus pitch between 1.4-2.4 and relative hole sizes larger than 0.6 was mapped out by Travers in [25], who defined the blue edge as the shortest GV matched wavelength, without relating it to the inherent material loss edge. Travers found that the optimum pitch was

#161502 - $15.00 USD Received 13 Jan 2012; revised 26 Mar 2012; accepted 18 Apr 2012; published 24 Apr 2012

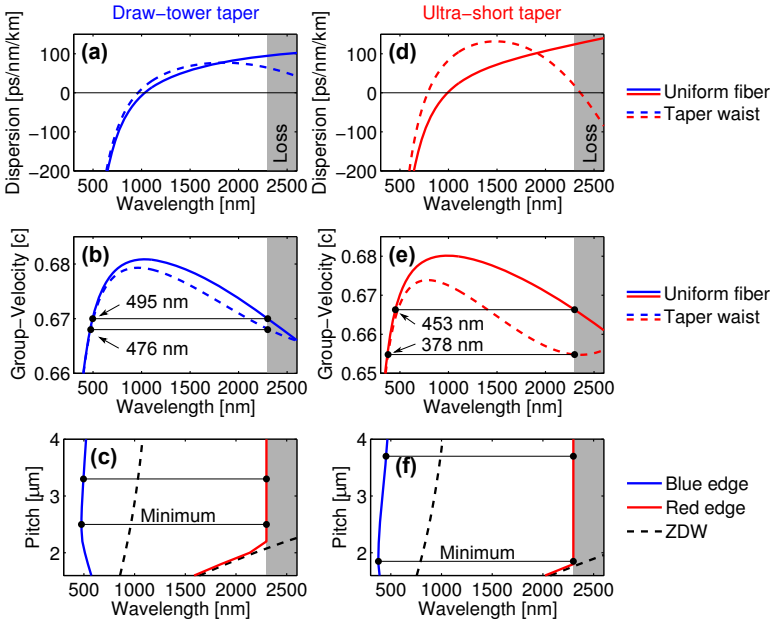


Fig. 3. (a) Dispersion and (b) GV for the draw-tower taper for the uniform fiber (solid line) and at the taper waist (dashed line). The shaded areas mark the loss region above 2300 nm where the soliton redshift halts, and the horizontal lines in (b) show the GV matching of the expected red edge to the blue edge for the uniform fiber and taper. (c) Blue edge (blue line), red edge (red line) and ZDWs (dashed lines) as a function of wavelength and pitch defined as described in the text. The horizontal lines are as in (b) and confirm that the shortest possible wavelength is reached in the taper. (d)-(f) show the same for the ultra-short tapers.

2 $\mu$m almost independently of the relative hole size and provided a qualitative explanation [25]. Introducing the loss edge has here allowed us to give a quantitative measure of the blue edge and an explanation of why the optimum pitch saturates close to 1.8 $\mu$m for large relative hole sizes.

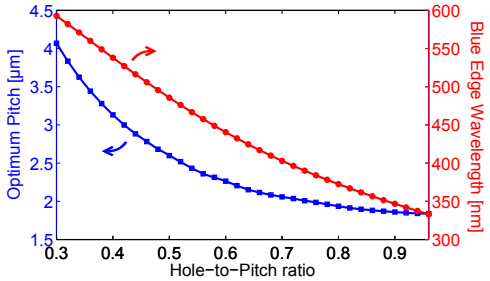


Fig. 4. Optimum pitch and corresponding minimum wavelength of the blue edge as a function of the fiber's hole-to-pitch ratio, calculated as described in the text by GV matching to the loss edge at 2300 nm or 50 nm below the second ZDW. For higher hole-to-pitch ratios the minimum wavelength is generally found for a pitch around 1.8 $\mu$m.

#161502 - $15.00 USD Received 13 Jan 2012; revised 26 Mar 2012; accepted 18 Apr 2012; published 24 Apr 2012

The fibers were pumped with a 1064 nm Yb fiber-laser typical for commercial SC sources. The laser emits 10 ps pulses with an average output power of 14 W at a repetition rate of 80 MHz. For the draw-tower taper, the fiber was spliced directly to the laser for maximum coupling efficiency and stability. For the ultra-short Vytran tapers the laser output was free-space coupled with an efficiency of approximately 70 %. In both cases the output was collimated and recorded with an optical spectrum analyser (OSA) through an integrating sphere. The output power was measured with a power meter and the spectra normalised accordingly. For the draw-tower taper the infrared edge was measured with an additional OSA and the two spectra were stitched together.

### *3.1. Draw-tower taper*

First we analyse the draw-tower taper. The taper profile was monitored during the fabrication by measuring the coating diameter. Figure 5(a) shows a final cutback measurement of the cross-section, which was carried out after the experiments had been performed. The images captured with an optical microscope confirm that the fiber's hole structure was maintained and a hole-collapse avoided. The measured coating diameter and pitch calculated from cross-sectional images are shown in Fig. 5(b). They are nicely correlated and show how the pitch is reduced from 3.3 to 2.5 $\mu$m in an asymmetric way that roughly can be described as a 1.5 m downtapering section and a 0.5 m uptapering section. The coating diameter can thus be used to get a good estimate of the taper profile. The hole-to-pitch ratio of 0.52 was preserved throughout the taper. In the experiment there was 5 m of uniform fiber before and after the tapered section to allow for an initial spectral broadening.

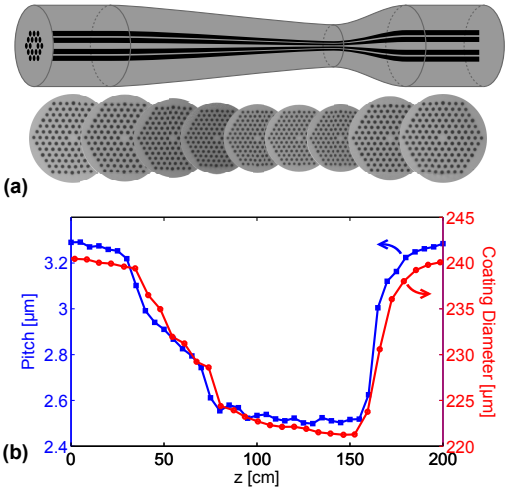


Fig. 5. Measured profile of the asymmetric draw-tower taper. (a) Schematic with cross-section images captured with an optical microscope at 100x magnification. The structure was maintained throughout the length of the taper. (b) Coating diameter and fiber pitch (hole spacing) calculated from cross-section images through the tapered section. The hole-to-pitch ratio of 0.52 was constant though the taper.

Figure 6(a) shows the spectra recorded when pumping from the long (blue) and short (red) downtapering sides. A reference spectrum from a 10 m uniform fiber (black) is included to show the maximum bandwidth achievable in a uniform fiber. Figures 6(b)-6(c) show a close up of the blue edge and the integrated power. It is clearly evident that pumping from the long downtapering side yields a higher power in the blue edge than pumping from the short. Both

#161502 - $15.00 USD Received 13 Jan 2012; revised 26 Mar 2012; accepted 18 Apr 2012; published 24 Apr 2012

spectra from the tapered fiber extend below the bandwidth achievable in the uniform fiber, as expected. These results confirm the importance of GAM: when the taper is too steep, the solitons at the red edge are decelerated too fast relative to the DWs at the blue edge. A fraction of the energy in the DWs hence escapes the trapping potentials from the solitons and is consequently not blueshifted. In the present taper, pumping from even the optimum long downtapering side gives only a small addition to the energy below 500 nm compared to the uniform fiber. However, the energy below the spectral edge of the uniform fiber is increased threefold from 12.8 to 37.7 mW when the taper is pumped from the long downtapering side.

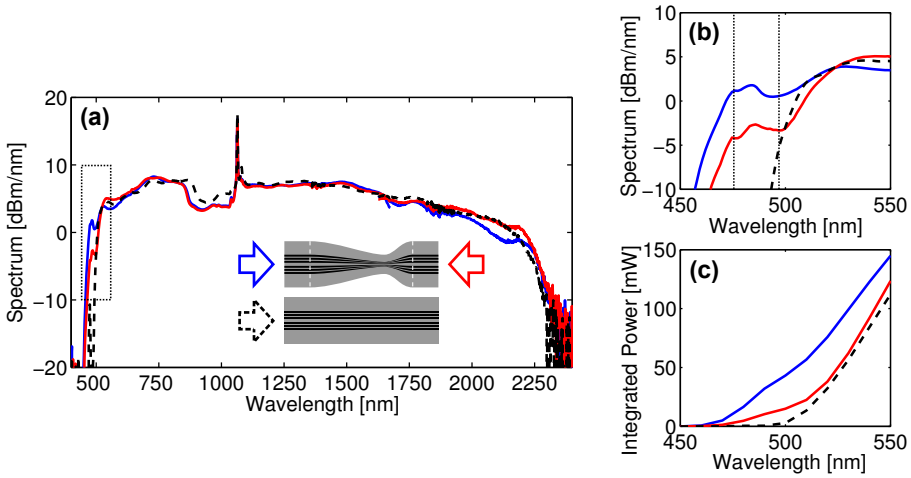


Fig. 6. Experimental output spectra of the asymmetric draw-tower taper. (a) Output spectra when pumping the taper from the long (blue) and short (red) downtapering sides. The spectrum of a 10 m uniform fiber (black dash) is shown for comparison. The insets show the pump directions. (b) Close up of the blue edge marked in (a), the vertical dotted lines mark the spectral edges calculated in Fig. 3(b). (c) Integrated power in the blue edge. Pumping from the long downtapering side clearly gives a higher power in the blue edge.

The prediction of the blue edge from Fig. 3(b)-3(c) is marked by vertical lines in Fig. 6(b). The agreement is best for the uniform fiber, which may be due to small changes in the hole-to-pitch ratio in the taper. Furthermore, determining the exact red edge is ambiguous in terms of the specific wavelength of the loss edge.

### *3.2. Ultra-short tapers*

For the ultra-short Vytran taperes the total fiber length was fixed to 50 cm with a 6 cm symmetrically tapered section in the middle. The tapers differed from each other in the length of the up and downtapering sections that was set to 30, 20 and 5 mm, respectively. This corresponds to waists of 0, 20 and 50 mm, respectively. The results shown in Fig. 7 again clearly confirm the importance of GAM: increasing the length of the downtapering section with just a few millimetres gives a dramatic increase in the power in the blue edge.

In Fig. 3(e)-3(f) we found that the blue edge should be at 453 and 378 nm for the uniform and tapered fiber, respectively. This, however, was found by assuming a red edge at 2300 nm, which can only be achieved by increasing the fiber length to allow the solitons to redshift all the way to the loss edge. The results for the ultra-short tapers nonetheless demonstrate that the blue edge can be easily shifted to much shorter wavelengths than what was demonstrated for the draw-tower taper by increasing the fiber's relative hole-size to alter the dispersion and GV

#161502 - $15.00 USD Received 13 Jan 2012; revised 26 Mar 2012; accepted 18 Apr 2012; published 24 Apr 2012

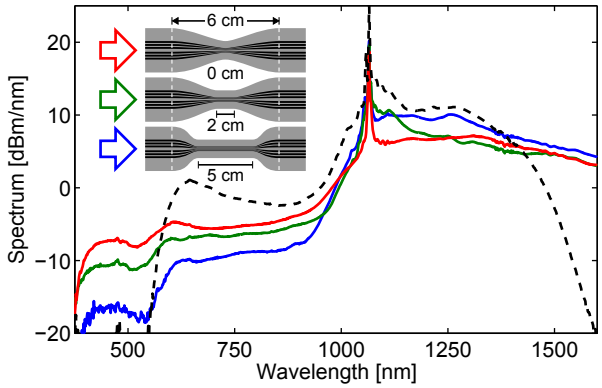


Fig. 7. Experimental spectra from ultra-short symmetrical tapers with increasing transition lengths: The blue, green and red lines show the spectra from tapers with increasing lengths of the downtapering section. The black dashed line shows the spectrum at the entrance of the tapers. A longer downtapering section again clearly increases the power in the blue edge.

profile as shown in Fig. 4 and predicted in [25]. Here our goal was to maximize the energy in the blue-edge and verify the importance of GAM. The conclusions can be straightforwardly applied to fibers with higher relative hole-sizes and thus make an important step in optimising the taper profile for SC sources with high power in the deep-blue.

## 4. Discussion

So far, we have ascribed the energy leakage of the DWs to GAM alone. However, we would like to point out that a taper can be viewed as a continuous perturbation of the solitons that causes them to oscillate and shed energy in order to remain fundamental solitons. This oscillatory behaviour and energy shedding is also seen in Fig. 2 although the effect is minor here. A decrease in the peak-power of a soliton will decrease the potential well around the DW and could therefore also explain why the soliton can not blueshift all the energy of a DW package thought a taper. The importance of this effect will strongly depend on the size of the perturbation, e.g., a very short taper will cause a large perturbation of the soliton and make it harder to remain a fundamental soltion.

For the fibers investigated here, the soliton period for the most redshifted solitons at the entrance of the taper is in the order of a few millimetres assuming a realistic soliton width of 10 fs. This length is very small compared to the length of the draw-tower taper, and the solitons should therefore propagate adiabatically without oscillating and shedding more energy than they would in a uniform fiber due to the Raman effect alone. However, for the ultra-short Vytran tapers the soliton period is comparable to the length of the taper, which will lead to a non-adiabatic propagation of the solitons. We thus expect that the dynamics observed in the draw-tower tapers is dominated by GAM, whereas the dynamics in the ultra-short tapers will be affected both by GAM and the non-adiabatic propagation of the solitons. We emphasize that both explanations give the same results, i.e., for a fixed taper length, the available power in the blue edge will increase with the length of the downtapering section.

#161502 - $15.00 USD Received 13 Jan 2012; revised 26 Mar 2012; accepted 18 Apr 2012; published 24 Apr 2012

## 5. Conclusion

In conclusion, we fabricated an asymmetric short draw-tower taper and verified experimentally the importance of the novel concept of *group-acceleration mismatch*, or GAM, on solitonic dynamics and the efficiency of SC generation. In particular, it was demonstrated that, for a fixed taper length, a longer downtapering section yields a higher power in the blue edge of the spectrum due to a correspondingly lower GAM. In the present case, the energy in the blue edge was tripled when the length of the downtapering section was increased from 0.5 to 1.5 m. The same tendencies were observed in three ultra-short symmetric tapers fabricated on a tapering station, but for these very short tapers other effects may also play a role. These results are highly important in the design of deep-blue SC sources with high power in the blue edge based on tapered fibers.

## Acknowledgments

We thank the Danish Agency for Science, Technology and Innovation for support of the project no. 09-070566.

#161502 - $15.00 USD Received 13 Jan 2012; revised 26 Mar 2012; accepted 18 Apr 2012; published 24 Apr 2012